The compound of baicalein, wogonin, and oroxylin-A inhibiting EMT in A549 cell line via PI3K/AKT-TWIST1- glycolysis pathway

Hui-Juan Cao[a]†, Wei Zhou[b]†, Xiao-Le Xian[a]†, Shu-Jun Sun[c], Pei-Jie Ding[a], Chun-Yu Tian[a], Fu-Ling Tian[a], Chun-Hua Jiang[a], Ting-Ting Fu[a], Shu Zhao[a], Jian-Ye Dai[b,d,e]*

a. Traditional Chinese Medicine College, North China University of Science and Technology, Tangshan 063210, China

b. School of Pharmacy, Lanzhou University, Lanzhou 730000, China

c. School of biology and food engineering, Fuyang Normal University, Fuyang 236037, China

d. State Key Laboratory of Natural Medicines, China Pharmaceutical University, Nanjing 210009, China

e. Collaborative Innovation Center for Northwestern Chinese Medicine, Lanzhou University, Lanzhou 730000, China

†These authors have contributed equally to this work and share first authorship

* Correspondence: Jianye Dai: daijy@lzu.edu.cn

Abstract:

Non-small cell lung cancer (NSCLC) is a worldwide disease with high morbidity and mortality, however, the epithelial-mesenchymal transition (EMT) process promotes cancer cell migration and invasion, leading to NSCLC metastasis. Total Flavonoid Aglycones Extract (TFAE) isolated from *Scutellaria baicalensis* was reported to inhibit tumor growth and induce apoptosis. In this study, we found that baicalein, wogonin, and oroxylin-A as the active compounds of TFAE present inhibitory effect on the EMT process of A549 cells. Then, network pharmacology technology was employed to elucidate the pharmacodynamic mechanism network of TFAE. We figured out the relationship between TFAE and PI3K/Akt signaling pathways, with TWIST1 as the key protein. LY294002, the inhibitor of PI3K/Akt signaling pathway, and knock-down TWIST1 could significantly enhance the efficacy of TFAE, and, at the same time, increase expression of epithelial markers and decrease expression of mesenchymal markers in A549 cells. Furthermore, chemical proteomic results showed that the EMT-inhibition process may be realized through glycolysis pathway.

Keywords: Total Flavonoid Aglycones Extract, Epithelial-mesenchymal transition, Network pharmacology, Stable isotope dimethyl-labeled proteomics technology, TWIST1, PI3K/Akt signaling pathway

1.Introduction

Lung cancer is a worldwide disease with high morbidity and mortality. According to World Health Organization[1], there were 2.207 million new lung cancer patients worldwide in 2020, only less than breast cancer; and lung cancer ranked first in the global causes of death. Among the histological subtypes of lung cancer collectively, non-small cell lung cancer (NSCLC) accounts for 80%-85%; and most lung cancer patients are diagnosed at advanced stages, so traditional chemotherapy and radiotherapy have limited efficacy[2]. NSCLC microenvironment has limited nutrition, so cancer cells often obtain the energy and substances required for proliferation and cell growth through the "Warburg Effect" glucose metabolism changes[3, 4], that is, cancer cells tend to produce energy through glycolysis rather than oxidative phosphorylation[5-7]. However, the metabolic change leads to further tumor cell growth, aggravation of epithelial-mesenchymal

transition (EMT) process and resistance to treatment. During the treatment of NSCLC, 40% of patients have metastases[8], and the main biological process is EMT [9]. In EMT process, cells gradually become spindle-shaped, losing the unique epithelial characteristics, intercellular adhesion and cytoskeletal structure of epithelial tissue, and possessing polarity, individual migration ability and invasion ability[10]. Cellular EMT process is related to TGFR, Wnt/β-Catanin, PI3K/Akt, Ras, MAPK, NF-κB pathways, and the transcription factors involved are TWIST (TWIST1 and TWIST2), Slug, ZEB (ZEB1 and ZEB2), Snail et al[11, 12].EMT transcription factors promote the development of drug resistance in tumor therapy and may become new targets for tumor therapy[13, 14] . In the process of EMT, the activated PI3K/Akt pathway promotes glucose uptake and glycolysis[15, 16], and phosphorylated Akt can phosphorylate TWIST1, then up-regulate the TGFβ-Smad pathway, which further promote the EMT process [17]. TWIST1 was known to bind to the E-box sequence of E-cadherin and inhibited the expression of E-cadherin to induce EMT in a variety of tumors [18-20].Inhibition of TWIST1 was known to induce growth inhibition and apoptosis of EGFR-mutant NSCLC cells[21].

Many traditional herbals and their extracts have been reported to have therapeutic effects on cancer, including *Scutellaria baicalensis* [22, 23], whose main components are flavonoids. Total Flavonoid Aglycones Extract (TFAE) isolated from *Scutellaria baicalensis* was reported to inhibit tumor growth and induce apoptosis, in which the main components, baicalein, wogonin, and oroxylin-A accounts for 41.4%, 13.3%, and 8.2%, respectively [24]. We demonstrated baicalein, wogonin, and oroxylin-A as the active compounds of *Scutellaria baicalensis* extract and named it as TFAE, through mass conversion, the proportions of the three components in TFAE are 65.8%, 21.2%, and 13.0%, respectively (Fig.1A). Considering the high metastasis of NSCLC [3], we studied the mechanism of TFAE inhibiting EMT of A549 cells.

In this study, TFAE was prepared according to the ratio of baicalein, wogonin, and oroxylin-A in the extracted total flavonoids of *Scutellaria baicalensis*, to explore its effect on the EMT process of A549 cells. Network pharmacology was performed to explore connections between TFAE and lung cancer. Inhibited PI3K-AKT pathway was considered as the key pathway for TFAE's EMT-inhibition. It was confirmed by the LY294002, inhibitor of PI3K-Akt, which had similar effects to TFAE. Furthermore, targets screening showed TWIST1 was the key protein, as knock-down TWIST1 could enhance the effect of TFAE in A549 cells. Wound healing assay and cell invasion assay were applied to monitor cell migration and invasion ability, and western blot was applied to detect the expression of EMT-related proteins. Cell experiments results showed that TFAE inhibited the EMT process of A549 cells through cell migration and invasion ability, and affected the expression of EMT-related proteins. Finally, stable isotope dimethyl-labeled proteomics was performed to illustrate how TFAE-inhibition of PI3K-Akt pathway affects the EMT process. Above all, we claimed that, when the PI3K/Akt pathway was inhibited, TWIST1 would be reduced. Then the expression of PKM, ALDOA, and GPI genes were affected, thereby inhibiting glycolysis and pentose phosphate signaling pathways, which finally inhibited the EMT process of A549 cells.

2.Materials and Methods

2.1. Cell culture

The A549 cells was obtained from the Cell Resource Center, Peking Union Medical College, and were cultured at 37 °C under 5 % CO_2 in Dulbecco's modified Eagle's medium (DMEM; Sigma, D6429) supplemented with 10% (vol./vol.) fetal bovine serum (FBS; Gibco, 10270-106), and 1 %

(vol./vol.) penicillin-streptomycin (PS; Gibco, 15140-122). Culture medium was refreshed and the cells were passaged when the confluency was 80%.

2.2. Preparation of cisplatin, LY294002 and TFAE

4mg/mL cisplatin stock solution, 20mM LY294002 stock solution and 128mg/mL TFAE solution were prepared by DMSO and were used for the later experiments. For TFAE, the three main components and their mass percentages are baicalein (65.8%), wogonin (21.2%), and oroxylin-A (13.0%). Weigh the amount of each TFAE component according to their mass percentage, then mix the three compounds, and dissolve them to the desired volume with DMSO.

2.3. Wound healing assay and cell invasion assay

For wound healing assay: $1.7*10^7$ A549 cells were plated in six-well plates. 7 hours later, the cells formed a single layer with nearly 100% confluency. A linear wound was made by scraping the confluent cell layer with a 200μL tip. Cells were washed with PBS for 3 times to remove detached cells and debris. Cells were incubated with complete medium with or without TFAE, Cisplatin, or LY294002 for 24 h. At 0 and 24h after scratching, 3 fields of view for each well were select randomly to take pictures. Image J software were used to scan the scratch areas and to calculate the wound healing area. Wound healing rate= (wound area at 0h- wound area at 24h)/ wound area at 0h *100%.

For cell invasion assay: the transwell containing polycarbonate membranes with 8μm pore size was precoated with 50μL of Matrigel(1.0mg/mL) and incubated at 37°C overnight. $1.0*10^6$ A549 cells and TFAE (2, 4, 8 μg/mL) in serum-free DMEM medium were plated in the upper chamber, followed by 150μL of serum-supplemented DMEM medium in the lower chamber. After 24h of incubation, the upper chamber was taken out and washed by wash buffer for 2 times, then was transferred to test board containing 100μL Cell Dissociation Solution/Calcein-AM. After 1h of incubation, the fluorescence value was detected at 485nm excitation wavelength and 520nm emission wavelength. Cell invasion rate= (number of invaded cells in experimental wells/ number of invaded cells in control wells) *100%.

2.4. Western blot

The A549 cells treated under different conditions were collected after washed by PBS for three times and centrifugation at 3000 rpm for 3 minutes. The cells were lysed in RIPA Lysis Buffer (CWBIO, CW2333S) containing EDTA-free cOmplete(Roche, 4693132001) with sonication on ice. The cell lysates were collected by centrifugation (150*100rpm, 20min) at 4°C. The protein concentration was detected by Pierce™ BCA Protein Assay Kit (Thermo Fisher Scientific, 23225) and adjusted to 2mg/mL.20μg of the lysates were separated by 10% SDS-PAGE and then transferred onto a PVDF membrane in an ice bath at 300mA for 1h. The membrane was blotted with 5% nonfat milk in TBST at RT for 1h and then incubated with the following antibodies at 4°C overnight: TWIST1(Cell Signaling Technology, 46702S), E-cadherin (Cell Signaling Technology, 3195), Vimentin (Cell Signaling Technology,5741), N-cadherin (Santa, Sc-59987), AKT (Cell Signaling Technology, 4685), p-AKT (Cell Signaling Technology, 4060), β-Actin (Proteintech, 20536-1-AP). GAPDH (Proteintech, 10494-1-AP). Then the membrane was incubated with secondary antibodies at RT for 1h. The secondary antibodies are as follows: Goat anti-Rabbit IgG (Proteintech, SA00001-2), Goat anti-mouse IgG (Proteintech, SA00001-1). Finally, the immunoreactive bands were visualized by the Clarity™ Western ECL Substrate (BIO-RAD,1705061) using the Tanon4600 Automatic chemiluminescence image analysis system (Tanon, Shanghai, China).

2.5. Transfection

$6.0*10^5$ A549 cells were plated in six-well plates. 7 hours later, the cells with nearly 70% confluency were transfected with TWIST1 siRNA. The siRNA sequences were as follows: TWIST1(sense:5'-CAAGAUUCAGACCCUCAAGTT-3', antisense:5'-CUUGAGGGUCUGAAUCUUGTT-3'); GAPDH (sense:5'- AATGGGCAGCCGTTAGGAAA -3', antisense: 5'- TGAAGGGGTCATTGATGGCA -3'). A siRNA nonspecific control was also used in this study. SiRNA sequences were designed and synthesized by GenePharma (Shanghai, China). The interference was performed based on the protocol of Lipofectamine® 3000 (Thermo Fisher Scientific). The silencing efficiency was examined by qRT-PCR.

2.6. Quantitative real-time PCR (qRT-PCR)

Total RNA was extracted and purified with Eastep® Super Total RNA Extraction Kit (Promega, LS1040) and used as the cDNA synthesis template for reverse transcription with the RevertAid First Strand cDNA Synthesis Kit (Thermo Scientific, k1622). The reverse transcription conditions were as follows: 42℃ 30min；85℃ 10min. qRT-PCR was performed by MX3000P(Agilent) using UltraSYBR Mixture (Low ROX) (CWBIO, CW2601), reaction conditions were :95℃ 3min; 95℃ 15s; 55℃ 30s, 72℃ 30s; 40 cycles. The primers were as follows: TWIST1(forward: 5'-TCGGACAAGCTGAGAGCAAGATTCA-3', reverse: 5'- TCCATCCTCCAGACCGAGAAGG -3'), GAPDH (forward: 5'- CATGAGAAGTATGACAACAGCCT-3', reverse: 5'-AGTCCTTCCACGATACCAAAGT-3'). CT values were used to evaluate the relative mRNA expression by $2^{-\Delta\Delta Ct}$ method and β-Actin served as an internal control. The primers were designed and synthesized by GenePharma (Shanghai, China).

2.7. Protein in-solution digestion and dimethyl labeling

A549 cells were grown to 80% confluence in 15cm dish. A549 cells were treated with 64μg/mL TFAE for 24h. The cells were collected after washed by PBS for three times and centrifugation at 3000 rpm for 3 minutes. The cells were lysed in 0.1% Triton X-100(Sigma-Aldrich, T8787)-100mM TEAB(Sigma-Aldrich, T7408) containing EDTA-free cOmplete with sonication on ice. The cell lysates were collected and the protein concentration was detected by Pierce™ BCA Protein Assay Kit. 10μL cell lysates(3mg/mL) were reacted with 30μL 8M urea and 2μL 200mM DTT at 65℃ for 15min in the dark. Then 2μL 400mM iodoacetamide was added to react in light for 30min at 35℃. 2μL 200mM DTT was added to react with the remaining iodoacetamide in light for 15min at 65℃. 100μL 100mM TEAB, 2μL 0.2μg/μL trypsin (Promega, V528A) and 1.5μL 100mM $CaCl_2$ were added and the trypsin digestion was performed at 37℃ overnight. For dimethyl labeling: for the control("light") group, the peptides were reacted with 6μL 4% CH_2O (Sigma-Aldrich, F1635) and 6μL 0.6M $NaBH_3CN$ (Sigma-Aldrich, 42077); for the TFAE ("heavy") group, the peptides were reacted with 6μL 4% $^{13}CD_2O$ (Sigma-Aldrich, 596388) and 6μL 0.6M $NaBD_3CN$(Sigma-Aldrich,190020). The reaction was incubated at 22℃ for 1h. The reaction was quenched by 24μL 1% ammonia and 12uL formic acid. The "light" and "heavy" samples were combined and the desalination was performed by Pierce™ C18 Tips (Thermo Scientific,87782).

2.8. LC-MS/MS analysis.

Samples were analyzed by LC-MS/MS on EasyNano-LC and Q Exactive series Orbitrap mass spectrometers (Thermo Fisher Scientific). In positive-ion mode, full-scan mass spectra were acquired over the m/z ratio from 350 to 1800 using the Orbitrap mass analyzer with mass resolution of 7000. MS/MS fragmentation is performed in a data-dependent mode, and the TOP

20 most intense ions are selected for MS/MS analysis with a resolution of 17500 under HCD's collision mode. The isolation window was 2.0 m/z units, the default charge was 2+,the ormalized collision energy was 28%, the maximum IT was 50ms , and dynamic exclusion, was 20.0s. Under +57.0215 Da' s cysteine modification, the LC-MS/MS data was analyzed by ProLuCID. The isotopic modifications were set as static modifications on the N-terminal of a peptide and lysines, and 28.0313 and 34.0631 Da were for light and heavy labeling, respectively. The CIMAGE software was applied for quantitation, Proteins with an average ratio(light/heavy) above 1.5 were selected for further KEGG analysis.

2.9. Network pharmacology and molecular docking analysis

In this study, based on network pharmacology, the common mechanism of TFAE in the treatment of lung cancer was studied. The active ingredients and related targets of TFAE were integrated from TCMSP, BATMAN-TAM, STP and Pubchem databases. The standard names of these targets were united by UniProt database. Targets of lung cancer were enriched through GeneCards, NCBI(Gene), Therapeutic Target Database, and DisGeNET(v7.0) databases. Then the intersection targets of TFAE and disease were obtained. The STRING network and the Cytoscape 3.7.2 were used to construct Protein-Protein-Interaction (PPI) network, the DAVID database was used to perform KEGG analysis. Then Cytoscape 3.6.1 was used to build "Ingredient-Target-Signal Pathway" network. After confirming the key protein and molecules, their 3D structures were obtained from RCSB PDB database and ZINK database, respectively. In AutoDock Tools, hydrogen atoms were added to, while water molecules and co-crystallized ligands were removed from the protein and molecules. Glide was selected to dock according to the previously reported active amino acid sites. The docking was performed by the AutoDock Vina software[10]. And PyMOL was used to visualize various conformations of the ligand and its different binding interactions with the receptor.

2.10. Statistical analysis.

Student's t-test was used to compare experimental data. We analyzed the data in GraphPad Prism (GraphPad Software), using the unpaired, two-tailed t-test module. Statistical significance was considered when a p value was below 0.05. $*p < 0.05$; $**p < 0.01$; $***p < 0.001$. N.S. not significant.

3.Results

3.1. TFAE inhibited EMT processes of A549 cells

To explore TFAE's effect of the EMT process on lung cancer, A549 cells were treated with TFAE (2, 4, 8 μg/mL) for 48 hours. Compared to 0μg/mL TFAE, the invasion rate of cells treated by TFAE concentration-dependently decreased (Fig.1B). In addition, TFAE dose-dependently inhibited the expression of TWIST1, p-AKT and N-cadherin proteins, while increased the expression of E-cadherin (Fig.1C). Compared with the wound area at 0 hours, the wound caused by tips were dose-dependently healed by TFAE(Fig.1D), which means TFAE inhibited the migration of A549 cells.

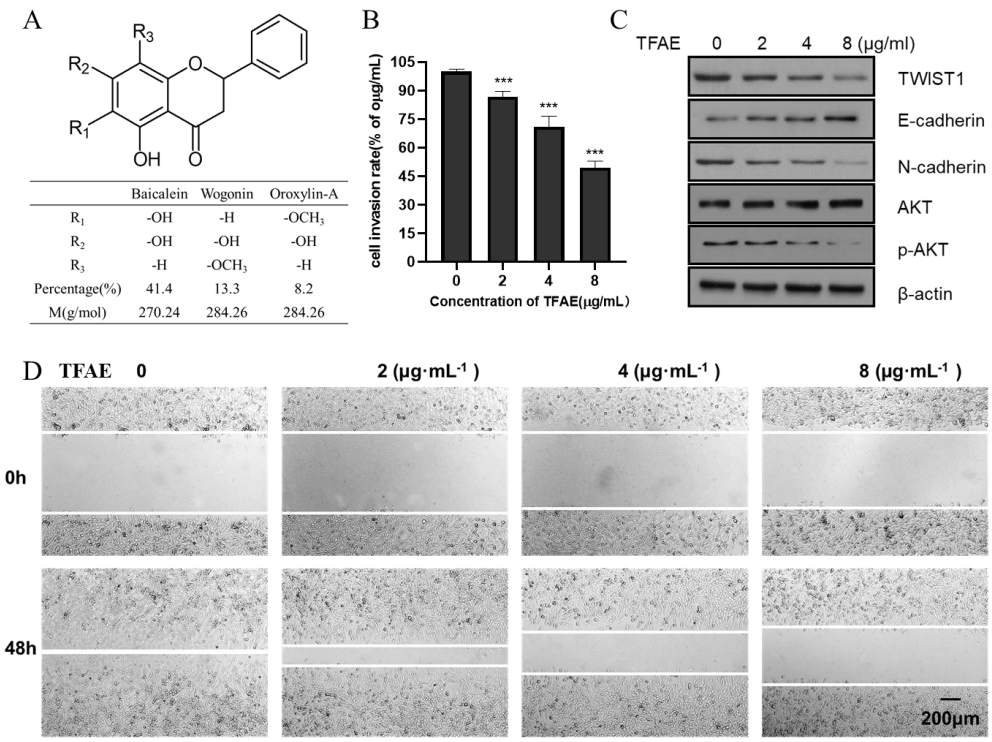

Fig.1 TFAE inhibited EMT process of A549 cells. (A) The structure and proportion of the main components of TFAE. (B) The invasion-inhibiting ability of TFAE on A549 cells. (C) Effects of different concentrations of TFAE on the expression of EMT-related proteins. (D)TFAE inhibits A549 cell migration. Statistical differences were determined by a two-sided Student's t-test. Compared with 0μg/mL TFAE, ***$P < 0.001$; **$P < 0.01$; *$P < 0.05$.

3.2. TFAE inhibited EMT process via PI3K/Akt pathway

The above results indicated that TFAE exerted a concentration-dependent inhibitory effect on the EMT process of A549 cells. To explore the connection between TFAE and lung cancer, network pharmacology analysis was performed. Three active ingredients and 65 related targets of TFAE were integrated from TCMSP, BATMAN-TAM, STP and Pubchem databases. 22474 targets of lung cancer were enriched through GeneCards, NCBI(Gene), Therapeutic Target Database, and DisGeNET(v7.0) databases. Venn diagram showed the intersection of 62 TFAE and lung cancer targets (Fig.2A). STRING network and Cytoscape 3.7.2 were used to construct Protein-Protein-Interaction (PPI) network (Fig.2B), AKT1 was the central protein. DAVID database was used to perform KEGG analysis, TFAE regulated pathways with P<0.01 were as follows: TNF signaling pathway, p53 signaling pathway, PI3K/Akt signaling pathway, VEGF signaling pathway, HIF-1 signaling pathway, MAPK signaling pathway (Fig.2C). After literature research, PI3K/Akt signaling pathway attracted our attentions, which could highly activate tumor metastasis and directly regulate the expression of TWIST1, one of the key markers in EMT [17]. To investigate whether TFAE affects the EMT process of A549 cells by acting on PI3K/Akt signaling pathway, we incubated A549 cells with the PI3K/Akt pathway inhibitor, LY294002. In this part, cisplatin was as positive control.

Compared with normal cells, inhibition of PI3K/Akt pathway showed poor migration and invasion capabilities (Fig.2D and 2E), and increased expression of E-cadherin and decreased expression of Vimentin, N-cadherin, TWIST1 and p-AKT (Fig.2F), which were related with EMT progress. Therefore, we believe that TFAE ameliorated the EMT process of A549 cells by inhibiting the PI3K/Akt signaling pathway.

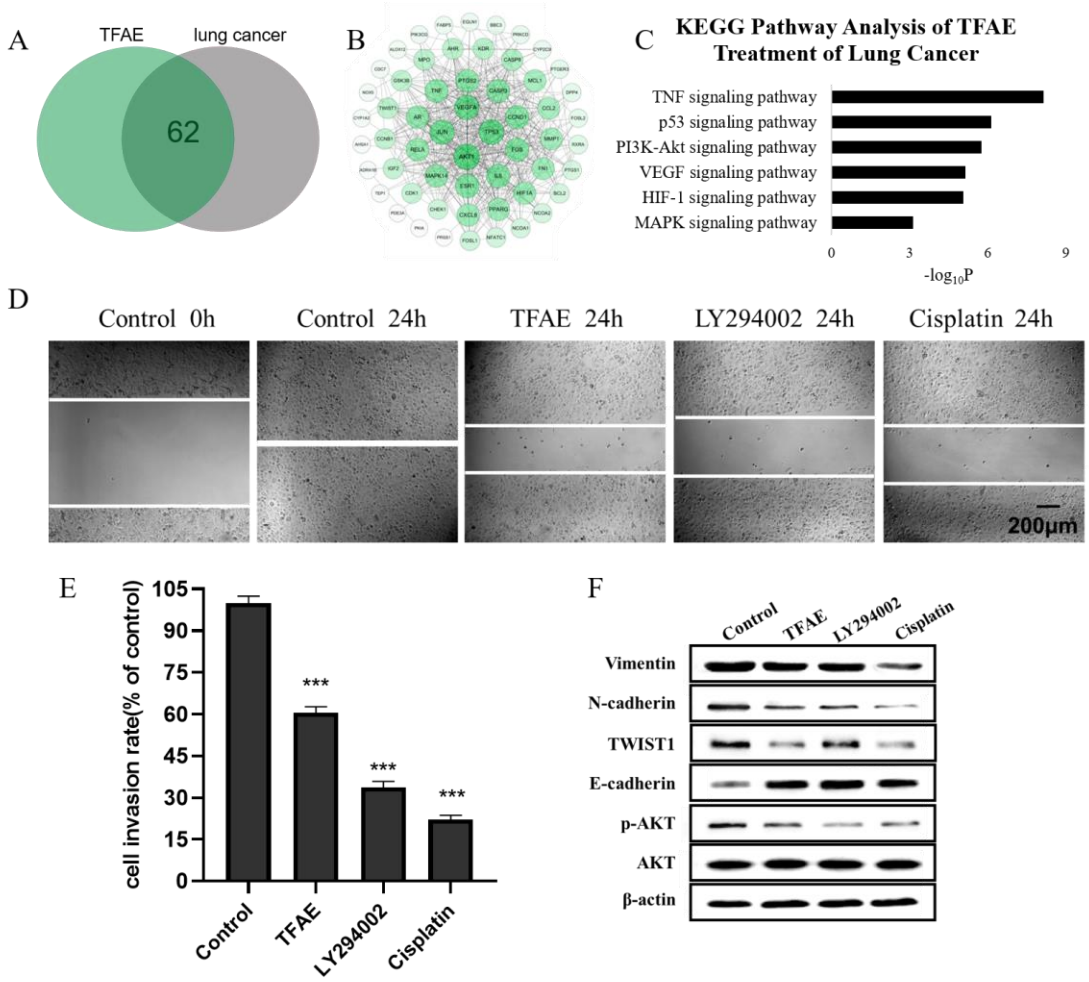

Fig.2 TFAE inhibited PI3K/Akt pathway to ameliorate EMT process of A549 cells. (A) Intersection protein targets of TFAE and lung cancer. 65 TFAE targets and 22474 lung cancer targets share 62 proteins. (B) Protein-Protein-Interaction (PPI) network of 62 proteins. AKT1, TP53, VEGFA, JUN show more connections with other proteins. (C) KEGG Pathway analysis of 62 proteins. P<0.01 was the cutoff for displaying the pathways. (D) The inhibition of PI3K/Akt-suppression and TFAE on wound healing. (E) The inhibition of PI3K/Akt-suppression and TFAE on A549 cell invasion. (F) The influence of PI3K/Akt-suppression and TFAE on the expression of EMT-related proteins. Statistical differences were determined by a two-sided Student's t-test. Compared with control, N.S., not significant, ***$P < 0.001$; **$P < 0.01$; *$P < 0.05$.

3.3. TFAE inhibited TWIST1 in EMT process of A549 cells

To identify the key target of TFAE, Cytoscape 3.6.1 was used to build "Ingredient-Target-Pathway" network. Among proteins involved in the network, TWIST1 attracted our attentions, which could be directly regulated by PI3K-Akt and connected with both baicalein and wogonin (Fig.3A). To investigate whether TWIST1 played an important role in TFAE's effect on the EMT process, we applied small interfering RNA (siRNA) method to knock down the TWIST1 gene in A549 cell.

Compared with normal cells, TWIST1-knockdowned A549 cells showed significant lower mRNA level(Fig.3B), and TFAE-treated/ siTWIST1 /TFAE&siTWIST1-treated cells showed poor migration and invasion capabilities, increased expression of epithelial marker(E-cadherin) and decreased expression of mesenchymal markers (Vimentin and N-cadherin), EMT-related

transcription factor (TWIST1) and protein in PI3K/Akt pathway(p-AKT) (Fig.3C and 3D). siTWIST1 showed similar effects to TFAE, and the synergistic application of TFAE and siTWIST1 showed more obvious effects (Fig.3E). Therefore, we claimed that TFAE inhibits the EMT process of A549 cells by inhibiting TWIST1.

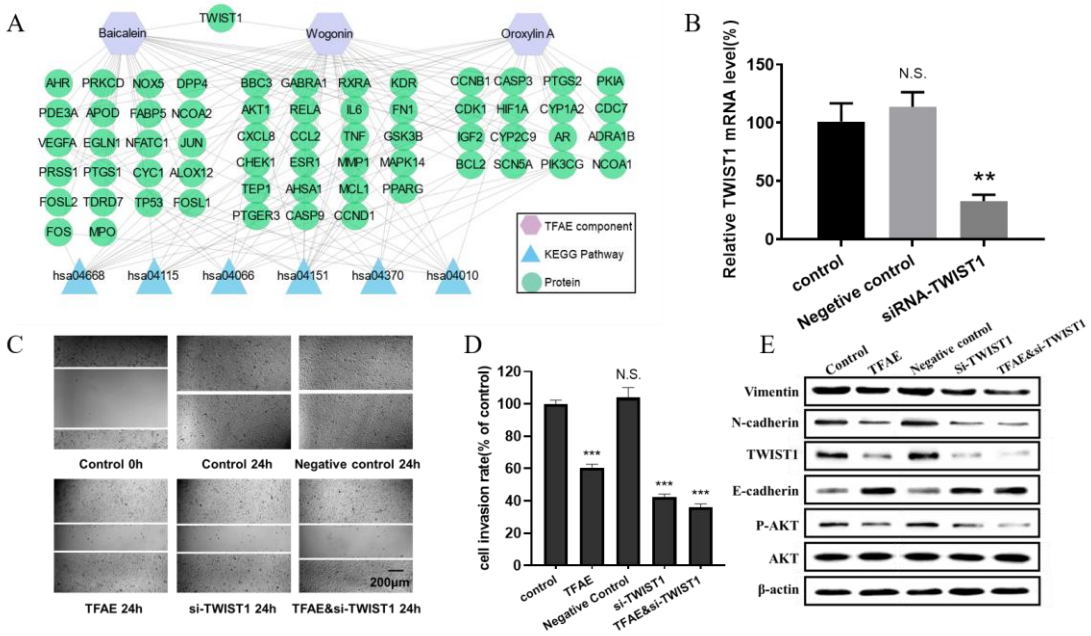

Fig.3 TFAE inhibited TWIST1 in EMT process of A549 cells. (A)Relationships of TFAE components-KEGG Pathways-Protein targets. (B)Relative TWIST1 mRNA level after siRNA interference. (C)The inhibitions of siTWIST1 and TFAE on wound healing. (D)The inhibitions of siTWIST1 and TFAE on A549 cell invasion rate. (E)The influence of siTWIST1 and TFAE on the expression of EMT-related proteins. Statistical differences were determined by a two-sided Student's t-test; Compared with control, N.S., not significant, ***$P < 0.001$; **$P < 0.01$; *$P < 0.05$.

3.4. The effect of TFAE on protein expression of A549 cells

We found that TFAE inhibited PI3K/Akt pathway and TWIST1 as above, yet it is not clear how TFAE led to the decline of EMT. To explain the further mechanism, we collected A549 cells treated with TFAE for 24 hours and performed stable-isotope dimethyl labeling proteomics experiment. The proteins of A549 cells treated with DMSO or TFAE were marked with "light" or "heavy", respectively, then mixed, desalted and analyzed by LC-MS/MS(Fig.4A). Proteins with Average Ratio Light/ Heavy(L/H)>1.5 were filtered out, and 158 proteins down-regulated by TFAE appeared at least twice in repeated experiments (Fig.4B). KEGG pathway analysis was performed on the 158 proteins and TFAE down-regulated pathways with P<0.01 were as follows: Carbon metabolism, Glycolysis/Gluconeogenesis, Biosynthesis of amino acid and Pentose phosphate pathway (Fig.4C). These four pathways contain 11, 9, 7, and 4 proteins respectively (Table1). In short, TFAE interferes with the sugar metabolism of A549 cells.

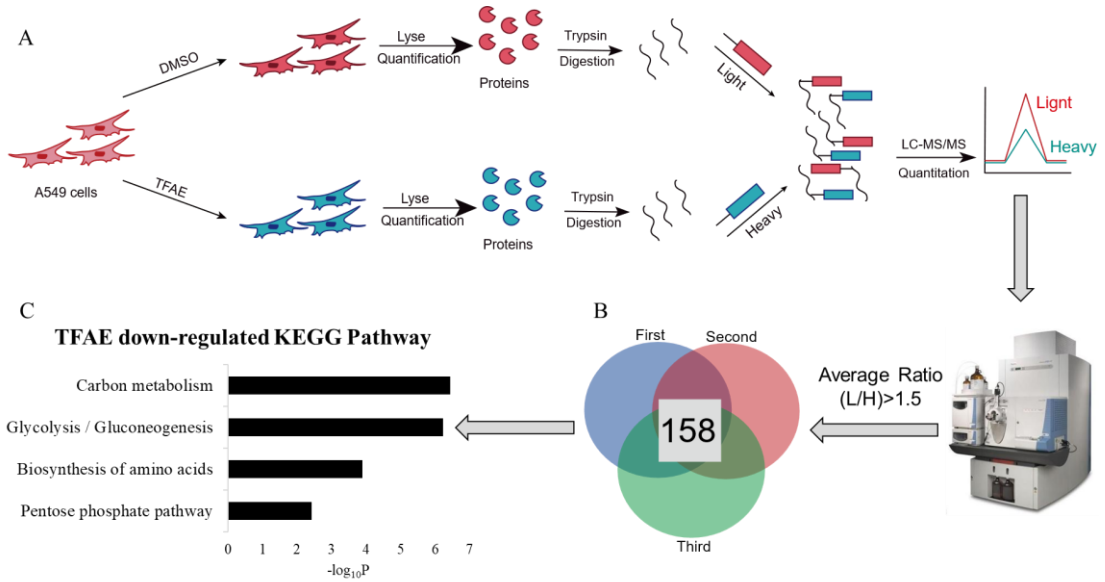

Fig.4 TFAE interfered with the glucose metabolism of A549 cells. (A)Overall scheme of In-solution dimethyl labeling experiment, the control or TFAE group were labeled with "light" or "heavy" respectively. (B) Venn diagram showing the 158 proteins with an averaged ratio >1.5 appeared twice of triple experiment. (C)KEGG Pathway analysis of the 158 proteins. P<0.01 was the cutoff for displaying the pathways.

Table1. Pathways interfered by TFAE, and proteins enriched in each pathway

Pathways	**Enriched Targets**
Carbon metabolism	GPI, PGAM1, PKM, HADHA, TALDO1, GAPDH, PGK1, MDH2, TPI1, ALDOA, G6PD
Glycolysis/Gluconeogenesis	GPI, PGAM1, PKM, LDHA, GAPDH, PGK1, TPI1, ALDH3A1, ALDOA
Biosynthesis of amino acid	PGAM1, PKM, TALDO1, GAPDH, PGK1, TPI1, ALDOA
Pentose phosphate pathway	GPI, TALDO1, ALDOA, G6PD

4.Discussion

The total flavonoids of *Scutellaria baicalensis* extract has an inhibitory effect on the EMT process of A549 cells, and may serve as an important breakthrough in the treatment of NSCLC[24]. In this study, we configured TFAE according to the ratio of the main components and found that it could inhibit the EMT process of A549 cells by affecting PI3K/Akt pathway and TWIST1. In detail, we firstly analyzed the possible mechanism of TFAE's effect on lung cancer and focused on PI3K/Akt pathway， which was confirmed by inhibition of LY294002 on PI3K/Akt pathway suppressing the migration and invasion of A549 cells, and causing high expression of epithelial-related protein and low expression of mesenchymal-related proteins. Then, network pharmacology analysis on the therapeutic effect of TFAE on lung cancer showed that TWIST1 was the common target of baicalein and wogonin. TWIST1 had been extensively studied in the EMT process, as shown below: the TWIST1-related axis may participate in the EMT process by activating the Wnt/β-catenin signaling pathway, thereby accelerating the process of lung cancer[25]. TWIST1 promotes EMT and metastasis through serine phosphorylation of p38, c-Jun N-terminal kinase (JNK) and Erk1/2[26]. The flavonoids target to and reduce the stability of TWIST1, thereby inhibiting the

process of NSCLC[27]. Therefore, TWIST1 is an important mediator in the process of cancer. TWIST1-targeted flavonoid provided a new strategy to inhibit EMT progress. In this study, “knockdown TWIST1” and “TFAE incubation” showed similar EMT-inhibition tendency, and the combined effect was more significant. In summary, we believe that TFAE inhibits PI3K/Akt pathway and TWIST1, thereby inhibiting the EMT process of A549 cells.

Stable-isotope dimethyl labeling proteomics results showed that TFAE down-regulated the carbon metabolism, glycolysis/gluconeogenesis, biosynthesis of amino acid, pentose phosphate pathway, etc. Tumor cells obtain energy mainly through the process of glycolysis, which promotes the EMT process of tumor cells[28]; when nutrients were depleted, cancer cells tend to obtain metabolic materials through the pentose phosphate pathway[29]. Studies had shown that TWIST1 can promote glycolysis process[30-32]. In this study, ALDOA and GPI were enriched in both glycolysis and pentose phosphate pathways, while PKM and LDHA in glycolysis (Table1.). The relationships between the above genes and the EMT process had been reported: PKM expresses pyruvate kinase and catalyzes the transfer of phosphorylation groups from phosphoenolpyruvate to ADP to generate ATP and pyruvate[33]. PKM is expressed in fetal tissues and cancers, and participates in the EMT process of human colon cancer cells [34]. PKM interacts with TGFβ-induced factor homeobox 2 (TGIF2) to inhibit the transcription of E-Cadherin[35]. Glucose-6-phosphate isomerase edited by GPI catalyzes the conversion of glucose-6-phosphate to fructose-6-phosphate. GPI can also be produced by cancer cells to promote the EMT process[36]. GPI promotes the EMT process of breast cancer cells by inhibiting miR-200 and inducing ZEB1/2[37].Silencing GPI promotes the transition of human lung fibroblasts from the mesenchymal to the epithelial state[38].ALDOA expresses fructose-bisphosphate aldolase A, which is involved in glycolysis and gluconeogenesis, and is also overexpressed in cancer[39]. ALDOA is highly expressed in lung squamous cell carcinoma (LSCC) and depletion of ALDOA in lung squamous carcinoma cells reduces cell motility capabilities [40]. Overexpression of ALDOA in colon cancer cells leads to the EMT progress[41].In pancreatic cancer and bladder cancer cells, ALDOA-silencing increases E-Cadherin and decrease N-Cadherin expression[42, 43]. Lactate dehydrogenase-A (LDHA) enzyme converts pyruvate into lactic acid. LDHA promotes the EMT process, but the specific mechanism is not clear[44, 45].

However, this study has limitations. Firstly, tumor cells are able to adapt to drug interventions, for example, cisplatin can be resistant in the treatment of NSCLC[27]. Therefore, whether TFAE has a long-lasting effect on NSCLC needs further study. Secondly, whether TFAE has a direct relationship with glycolysis or PI3K/Akt-related proteins needs further verification. Thirdly, all experiments were carried out in cells, next we will perform animal experiments.

Moreover, we also explored the effects of the three main components of TFAE-baicalein, wogonin, and oroxylin-A on the EMT process, and found that baicalein had the most significant inhibitory effect on the EMT process of A549 cells, closing to the effect of TFAE. Next, we will explore the inhibitory mechanism of baicalein on NSCLC.

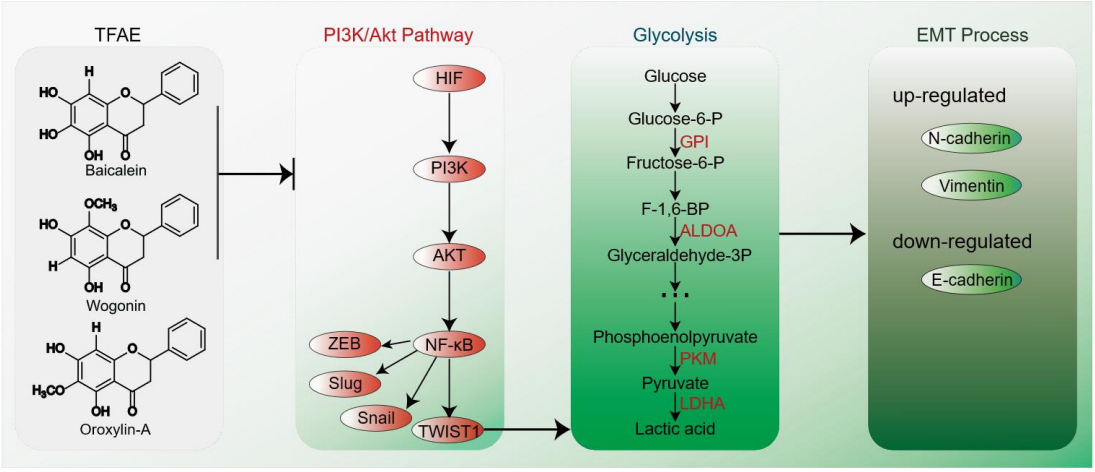

Fig.5 EMT process induced by TFAE. Baicalein and wogonin inhibit the PI3K/Akt pathway, thereby inhibiting TWIST1, which inhibits the glycolysis pathway and inhibits the EMT process of A549 cells.

5. Summary

In this work, we first determined that TFAE composed of three compounds in a definite proportion had the activity of inhibiting the invasion and metastasis of lung cancer A549 cells. Then combing with network pharmacology and molecular biology technology, PI3K-AKT-TWIST1 axis was inhibited by TFAE to ameliorate EMT progress. Furthermore, chemoproteomics was used to elucidate the changes of downstream protein networks after TFEA inhibited PI3K-AKT-TWIST1 axis, and it was found that glycolysis pathway may play an important role. In summary, TFAE can inhibit the PI3K/Akt pathway with the core of TWIST1, thereby inhibiting the glycolytic pathway to suppress EMT in A549 cells (Fig.5). TWIST1-targeted flavonoid provided a new strategy to inhibit EMT progress for the treatment of NSCLC.

6.Acknowledgement

This work is funded by the Science and Technology Project of Hebei Education Department (QN2018060), National Key Research and Development Program of China (2018YFC1706300 and 2018YFC17063005), the Science and Technology Planning Project of Gansu Province (20JR10RA586), the Fundamental Research Funds for the Central Universities(lzujbky-2021-kb40), the Project for Longyuan Youth Innovation and Entrepreneurship Talent.

7.References

1. *2020 World Health Statistics*. 2020 2020; Available from: https://www.who.int/data/collections.
2. MPH, R.L.S., et al., *Cancer Statistics, 2017.* Ca-Cancer J. Clin., 2017. **67**: p. 7–30.
3. Lopez-Lazaro, M., *The Warburg Effect: Why and How Do Cancer Cells Activate Glycolysis in the Presence of Oxygen?* Anti-Cancer Agents Med. Chem., 2008. **8**: p. 305-312.
4. Gatenby, R.A. and R.J. Gillies, *Why do cancers have high aerobic glycolysis?* Nat. Rev. Cancer, 2004. **4**: p. 891-899.
5. Heiden, M.G.V., L.C. Cantley, and C.B. Thompson, *Understanding the Warburg Effect: The Metabolic Requirements of Cell Proliferation.* Science, 2009. **324**: p. 1029-1033.
6. Muz, B., et al., *The role of hypoxia in cancer progression, angiogenesis, metastasis, and resistance to therapy.* Hypoxia, 2015. **2015**: p. 83-92.

7. Eales, K.L., K.E.R. Hollinshead, and D.A. Tennant, *Hypoxia and metabolic adaptation of cancer cells.* Oncogenesis, 2016. **5**: p. e190.
8. Keith, R.L., *Lung carcinoma.* 2017(https://www.msdmanuals.com/professional/pulmonary-disorders/tumors-of-the-lungs/lung-carcinoma.%20Accessed%20Nov%208,%202017.).
9. Tulchinsky, E., et al., *EMT: A mechanism for escape from EGFR-targeted therapy in lung cancer.* BBA-Rev. Cancer, 2018. **1871**: p. 29–39.
10. Trott, O. and A.J. Olson, *AutoDock Vina: Improving the speed and accuracy of docking with a new scoring function, efficient optimization, and multithreading.* J. Comput. Chem., 2010. **31**: p. 455–461.
11. T, S.A. and S. Benjamin, *Targeting anaplastic lymphoma kinase in lung cancer.* Clin. Cancer Res., 2011. **17**: p. 2081-2086.
12. Otsuki, Y., H. Saya, and Y. Arima, *Prospects for new lung cancer treatments that target EMT signaling.* Dev. Dyn., 2018. **247**: p. 462-472.
13. Tieju, L., et al., *The EMT transcription factor, Twist1, as a novel therapeutic target for pulmonary sarcomatoid carcinomas.* Int. J. Mol. Sci., 2020. **56**: p. 750-760.
14. Jente, v.S., et al., *Epithelial-mesenchymal-transition-inducing transcription factors: new targets for tackling chemoresistance in cancer?* Oncogene, 2018. **37**: p. 6195-6211.
15. L, S.G., *HIF-1: upstream and downstream of cancer metabolism.* Curr. Opin. Genet. Dev., 2010. **20**: p. 51-56.
16. Tennant, D.A., R.V. Durán, and E. Gottlieb, *Targeting metabolic transformation for cancer therapy.* Nat. Rev. Cancer, 2010. **10**: p. 267-277.
17. Gongda, X., et al., *Akt/PKB-mediated phosphorylation of Twist1 promotes tumor metastasis via mediating cross-talk between PI3K/Akt and TGF-β signaling axes.* Cancer Discovery, 2012. **2**: p. 248-259.
18. Ding, X., F. Li, and L. Zhang, *Knockdown of Delta-like 3 restricts lipopolysaccharide-induced inflammation, migration and invasion of A2058 melanoma cells via blocking Twist1-mediated epithelial-mesenchymal transition.* Life Sci., 2019. **226**: p. 149-155.
19. Hong, R., et al., *TWIST1 and BMI1 in Cancer Metastasis and Chemoresistance.* J. Cancer, 2016. **7**: p. 1074-1080.
20. Qing-Qing, Z., et al., *The role of TWIST1 in epithelial-mesenchymal transition and cancers.* Tumor Biol., 2016. **37**: p. 185-197.
21. Yochum, Z.A., et al., *Targeting the EMT transcription factor TWIST1 overcomes resistance to EGFR inhibitors in EGFR- mutant non-small-cell lung cancer.* Oncogene, 2019. **38**: p. 656-670.
22. P, C., et al., *Plasma concentrations of VCAM-1 and ICAM-1 are elevated in patients with Type 1 diabetes mellitus with microalbuminuria and overt nephropathy.* Diabetic Med., 2000. **17**: p. 644-649.
23. Dorota, W., D. Andrzej, and M. Adam, *Antiradical and antioxidant activity of flavones from Scutellariae baicalensis radix.* Nat. Prod. Res., 2015. **29**: p. 1567-1570.
24. Yang, W., et al., *Total flavonoid aglycones extract in Radix scutellariae inhibits lung carcinoma and lung metastasis by affecting cell cycle and DNA synthesis.* J. Ethnopharmacol., 2016. **194**: p. 269-279.
25. Pan, J., et al., *lncRNA JPX/miR-33a-5p/Twist1 axis regulates tumorigenesis and metastasis of lung cancer by activating Wnt/β-catenin signaling.* Mol. Cancer, 2020. **19**.
26. Jun, H., et al., *Phosphorylation of serine 68 of Twist1 by MAPKs stabilizes Twist1 protein and*

promotes breast cancer cell invasiveness. Cancer Res., 2011. **71**: p. 3980-3990.

27. Yuan, T., et al., *A natural product atalantraflavone inhibits non-small cell lung cancer progression via destabilizing Twist1.* Fitoterapia, 2019. **137**: p. 104275.
28. Liberti, M.V. and J.W. Locasale, *Correction to: 'The Warburg Effect: How Does it Benefit Cancer Cells?'.* Trends Biochem. Sci., 2016. **41**: p. 211-218.
29. Ilias, G.-S., et al., *EMT Factors and Metabolic Pathways in Cancer.* Front Oncol, 2020. **10**.
30. Sara, L., et al., *Endothelial-to-mesenchymal transition compromises vascular integrity to induce Myc-mediated metabolic reprogramming in kidney fibrosis.* Sci. Signaling, 2020. **13**: p. eaaz2597.
31. Li, Y., et al., *Twist promotes reprogramming of glucose metabolism in breast cancer cells through PI3K/AKT and p53 signaling pathways.* Oncotarget, 2015. **6**: p. 25755-25769.
32. Wang, X.-X., et al., *TWIST1 transcriptionally regulates glycolytic genes to promote the Warburg metabolism in pancreatic cancer.* Exp. Cell Res., 2020. **386**: p. 111713.
33. Dombrauckas, J.D., B.D. Santarsiero, and A.D. Mesecar, *Structural basis for tumor pyruvate kinase M2 allosteric regulation and catalysis.* Acta Crystallogr., Sect. A: Found. Crystallogr., 2005. **61**: p. 9417-9429.
34. Wong, N., et al., *PKM2 contributes to cancer metabolism.* Cancer Lett., 2015. **356**: p. 184-191.
35. Hamabe, A., et al., *Role of pyruvate kinase M2 in transcriptional regulation leading to epithelial–mesenchymal transition.* Proc. Natl. Acad. Sci., 2014. **111**: p. 15526-15531.
36. Y, N., et al., *Expression and secretion of neuroleukin/phosphohexose isomerase/maturation factor as autocrine motility factor by tumor cells.* Cancer Res., 1998. **58**: p. 2667-2674.
37. Tatsuyoshi, F., H. Victor, and R. Avraham, *Phosphoglucose isomerase/autocrine motility factor mediates epithelial and mesenchymal phenotype conversions in breast cancer.* Cancer Res., 2009. **69**: p. 5349-5356.
38. Tatsuyoshi, F., et al., *Down-regulation of phosphoglucose isomerase/autocrine motility factor results in mesenchymal-to-epithelial transition of human lung fibrosarcoma cells.* Cancer Res., 2007. **67**: p. 4236-4243.
39. Yu-Chan, C., et al., *Roles of Aldolase Family Genes in Human Cancers and Diseases.* Trends Endocrinol. Metab., 2018. **29**: p. 549-559.
40. Du, S., et al., *Fructose-Bisphosphate Aldolase A Is a Potential Metastasis-Associated Marker of Lung Squamous Cell Carcinoma and Promotes Lung Cell Tumorigenesis and Migration.* PLoS One, 2014. **9**: p. e85804.
41. Feng, Y., et al., *Aldolase A overexpression is associated with poor prognosis and promotes tumor progression by the epithelial-mesenchymal transition in colon cancer.* Biochem. Biophys. Res. Commun., 2018. **497**: p. 639-645.
42. Ji, S., et al., *ALDOA functions as an oncogene in the highly metastatic pancreatic cancer.* Cancer Lett., 2016. **374**: p. 127-135.
43. Jianwei, L., et al., *ALDOLASE A regulates invasion of bladder cancer cells via E-cadherin-EGFR signaling.* J. Cell. Biochem., 2019: p. 13694-13705.
44. Tirpe, A.A., et al., *Hypoxia: Overview on Hypoxia-Mediated Mechanisms with a Focus on the Role of HIF Genes.* Int. J. Mol. Sci., 2019. **20**: p. 6140.
45. Hou, X.-m., et al., *LDH-A promotes malignant behavior via activation of epithelial-to-mesenchymal transition in lung adenocarcinoma.* Biosci. Rep., 2019. **39**: p. BSR20181476.